

Supplementary Material

An overview of remote sensing data applications in peatland research based on works from the period 2010–2021

Sebastian Czapiewski ^{1,*} and Danuta Szumińska ²

¹ Institute of Geography, Kazimierz Wielki University, pl. Kościeleckich 8, 85-033 Bydgoszcz, Poland; sebastian.czapiewski@ukw.edu.pl, ORCID: <https://orcid.org/0000-0001-8010-1378>

² Institute of Geography, Kazimierz Wielki University, pl. Kościeleckich 8, 85-033 Bydgoszcz, Poland; dszum@ukw.edu.pl, ORCID: <https://orcid.org/0000-0001-7142-9080>

* Correspondence: sebastian.czapiewski@ukw.edu.pl

The development of satellite remote sensing commenced in 1972, i.e. with the launch of the ERTS-1 (Earth Resources Technology Satellite) system by NASA – now Landsat 1 [1]. However, the use of satellite remote sensing data did not gain momentum until the beginning of the 21st century, which may be attributed to the commissioning of systems capable of providing higher spatial resolution, such as IKONOS-2 and Landsat 7 [2]. The USGS announced the free-and-open data policy on 21 April 2008, rendering Landsat images free to the public [3]. As far as studies on peatland areas are concerned, the applicability of remote sensing data greatly improved with the launch of Landsat 8 in 2013, Sentinel-1A in 2014 and Sentinel-2A in 2015. In the following years, the European Space Agency launched twin satellites of the Sentinel 1 and 2 system, effectively reducing their revisit capability by half. Another multispectral satellite of the Landsat system was launched in September 2021 (Landsat 9 – currently undergoing tests) [4]. The European Space Agency plans to launch another 4 satellites operating in the Sentinel 1 and 2 system in the coming years, which is aimed at further enhancing the revisit capability [5,6]. Table S1 presents the characteristics of selected remote sensing data developed in 21st century, and Figure S1 demonstrates the multispectral range of Landsat 7-8 and Sentinel-2 satellite systems. Table S2 includes detailed information pertaining to the works analyzed in this study.

Citation: Czapiewski, S.; Szumińska, D. An overview of remote sensing data applications in peatland research based on works from the period 2010–2021. *Land* **2022**, *11*, 24. <https://doi.org/10.3390/land11010024>

Academic Editor: Daniel S. Mendham

Received: 29 October 2021

Accepted: 22 December 2021

Published: 24 December 2021

Publisher's Note: MDPI stays neutral with regard to jurisdictional claims in published maps and institutional affiliations.



Copyright: © 2021 by the authors. Licensee MDPI, Basel, Switzerland. This article is an open access article distributed under the terms and conditions of the Creative Commons Attribution (CC BY) license (<https://creativecommons.org/licenses/by/4.0/>).

Platform	Type of data	Launch date	Revisit capability
SPOT 5 [7]	<u>Multispectral</u> High Resolution Geometric (HRG) High Resolution Stereoscopic (HRS) Vegetation-2 Doppler Orbitography and Radiopositioning Integrated by Satellite (DORIS)	4 May 2002	5 days with two-satellite constellation (SPOT 4 and SPOT 5)
SPOT 6 [8]	<u>Multispectral</u> New AstroSat Optical Modular Instrument (NAOMI)	9 September 2012	between 1 and 3 days with only one satellite
Landsat 8 [1]	<u>Multispectral</u> Operational Land Imager (OLI) Thermal Infrared Sensor (TIRS)	11 February 2013	15 days
Sentinel-1A [5]	<u>Radar</u> Synthetic Aperture Radar (SAR)	3 April 2014	- 12 days - 3 days at the equator
Sentinel-2A [6]	<u>Multispectral</u> MultiSpectral Instrument (MSI)	23 June 2015	10 days
SPOT 7 (Azersky) [9]	<u>Multispectral</u> New AstroSat Optical Modular Instrument (NAOMI)	30 June 2014	- 1 day with SPOT 6 and SPOT 7 operating simultaneously - between 1 and 3 days with only one satellite - 10 days - 6 days out of phase with Senti-nel-1A - < 1 days at high latitudes out of phase with Senti-nel-1A
Sentinel-1B [5]	<u>Radar</u> Synthetic Aperture Radar (SAR)	25 April 2016	- 10 days - 6 days out of phase with Senti-nel-1A - < 1 days at high latitudes out of phase with Senti-nel-1A
Sentinel-2B [6]	<u>Multispectral</u> MultiSpectral Instrument (MSI)	7 March 2017	- 6 days out of phase with Sentinel-2A
Landsat 9 [4]	<u>Multispectral</u> Operational Land Imager 2 (OLI-2) Thermal Infrared Sensor 2 (TIRS-2)	27 September 2021	- 15 days - 8 days out of phase with Landsat-8

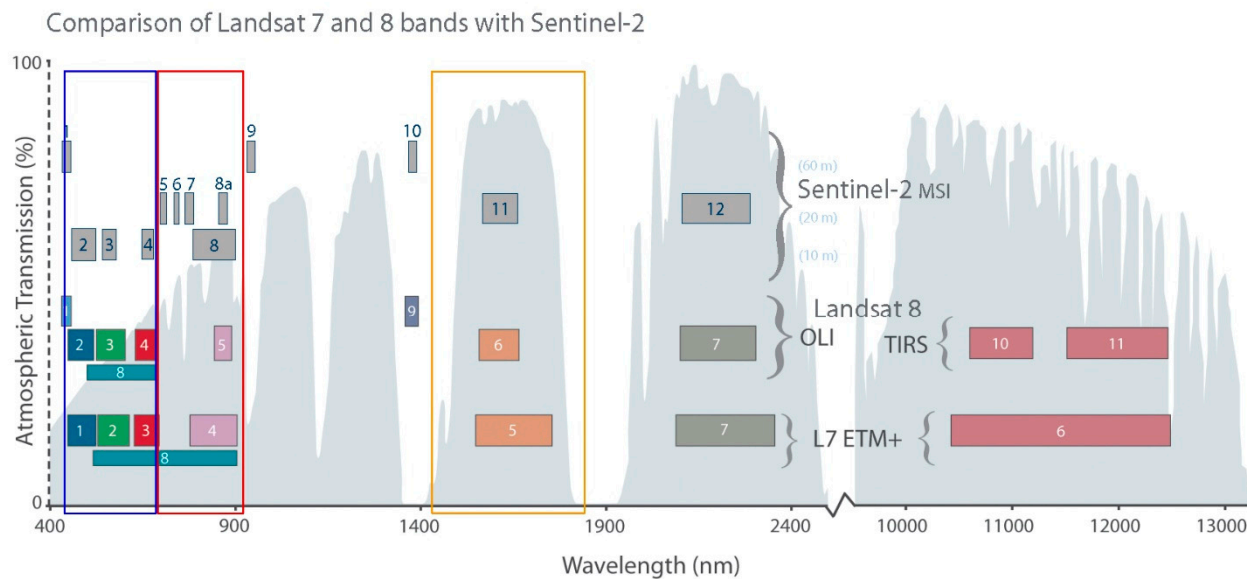


Figure S1. Multispectral range of Landsat 7-8 and Sentinel-2 satellite systems [10].

Table S2. Characteristics of reviewed studies.

Authors	Year	Location	Region	Used research methods	Platform	Type of data	The main focus of the research
Anderson et al. [11]	2010	Cumbria (UK)	oceanic temperate	Supervised classification	IKONOS	Multispectral	land classification / identification of peatlands changes in water conditions in the peatland
Miettinen and Liew [12]	2010	Indonesia	tropical	Vegetation indices Soil moisture indices	Landsat 5 SPOT	Multispectral	monitoring of peatland state
Neta et al. [13]	2010	Canada	boreal/northern	Water indices Vegetation indices	Airborne data	Hyperspectral	peatland vegetation mapping changes in water conditions in the peatland
Wijaya et al. [14]	2010	Borneo	tropical	Supervised classification	TerraSAR X Landsat	Multispectral Radar	land classification / identification of peatlands
Connolly et al. [15]	2011	Ireland	oceanic temperate	Vegetation indices	MODIS	Multispectral	monitoring of peatland state
Frick et al. [16]	2011	German	temperate	Vegetation indices Soil moisture indices	QuickBird WorldView I SPOT 2	Multispectral	peatland vegetation mapping changes in water conditions in the peatland
Harris and Dash [17]	2011	Canada	temperate/northern	Gross Primary Productivity	MODIS	Hyperspectral	estimating CO ₂ balance

							Gross Primary Productivity
Jaenicke et al. [18]	2011	Indonesia	tropical	Soil moisture indices	ASAR PALSAR	Radar	changes in water conditions in the peatland
Middleton et al. [19]	2012	Finland	boreal/northern	Soil moisture indices Machine learning land cover classification	Airborne data	Hyperspectral	peatlands classification
Miettinen et al. [20]	2012	Indonesia	tropical	Supervised classification	SPOT Landsat	Multispectral	estimating carbon resources in peatlands
Torbick et al. [21]	2012	Sweden	arctic	Water table depth (WTD) Supervised classification	PALSAR	Radar	land classification / identification of peatlands changes in water conditions in the peatland
Akumu and McLaughlin [22]	2014	Canada	temperate/northern	Supervised classification	SPOT 5	Multispectral	estimating carbon resources in peatlands
O'Connell et al. [23]	2014	Ireland	oceanic temperate	Vegetation indices	ASTER Landsat SPOT Ikonos QuickBird	Multispectral	peatland vegetation mapping
Watts et al. [24]	2014	Arctic circle	arctic	Gross Primary Productivity	MODIS	Hyperspectral	estimating CO2 balance Gross Primary Productivity
Cabezas et al. [25]	2015	Chile	temperate/oceanic	Vegetation indices Gross Primary Productivity	Landsat 8 Pleiades 1B	Multispectral	estimating carbon resources in peatlands
Crichton et al. [26]	2015	Cumbria (UK)	oceanic temperate	Supervised classification	Landsat Ikonos	Multispectral	estimating carbon resources in peatlands
Harris et al. [27]	2015	Wales (UK)	oceanic temperate	Vegetation indices	Airborne data	Hyperspectral	peatland vegetation mapping
Lehmann et al. [28]	2016	South Patagonia (Argentina) (Ar- grntina)	temperate/oceanic	Supervised classification	UAV (drone)	Multispectral	estimating carbon resources in peatlands
Bourgeau-Chavez et al. [29]	2017	Canada	boreal/northern	Supervised classification Machine learning land cover classification	Landsat 5 PALSAR	Multispectral Radar	peatlands classification

Connolly and Holden [30]	2017	Ireland	oceanic temperate	Supervised classification	QuickBird MODIS	Multispectral	land classification / identification of peatlands changes in water conditions in the peatland
Dissanska et al. [31]	2017	Canada	temperate/northern	Supervised classification	QuickBird	Multispectral	land classification / identification of peatlands
Erudel et al. [32]	2017	France	temperate	Vegetation indices	-	Hyperspectral	peatland vegetation mapping
Gatis et al. [33]	2017	Southwest England	oceanic temperate	Vegetation indices Supervised classification	MODIS	Multispectral	estimating carbon resources in peatlands peatland vegetation mapping
Gumbrecht et al. [34]	2017	-	tropical	Water indices Soil moisture indices	MODIS	Multispectral	land classification / identification of peatlands
Hribljan et al. [35]	2017	Ecuador	tropical	Supervised classification	Landsat PALSAR RADARSAT	Multispectral Radar	land classification / identification of peatlands estimating carbon resources in peatlands
Medvedeva et al. [36]	2017	Russia	temperate	Supervised classification	SPOT 5 SPOT 6 Landsat 7	Multispectral	monitoring of peatland state changes in water conditions in the peatland
Merchant et al. [37]	2017	Canada	boreal/northern	Supervised classification Machine learning land cover classification	RADARSAT-2	Radar	land classification / identification of peatlands
Novresiandi and Nagasawa [38]	2017	Malesia	tropical	Supervised classification	PALSAR Landsat 5	Multispectral Radar	land classification / identification of peatlands
White et al. [39]	2017	Canada	temperate/northern	Supervised classification	RADARSAT-2	Radar	land classification / identification of peatlands
Alshammary et al. [40]	2018	Northern Scotland (UK)	boreal/northern	InSAR ground deformation	Sentinel-1 ERS	Radar	monitoring of peatland state
Arroyo-Mora et al. [41]	2018	Canada	temperate/northern	Vegetation indices	Sentinel-2	Multispectral	peatland vegetation mapping
Kalacska et al. [42]	2018	Canada	temperate/northern	Water indices	Landsat 5 Landsat 8 Sentinel-2	Multispectral	changes in water conditions in the peatland

Marshall et al. [43]	2018	Malesia	tropical	InSAR ground deformation	Sentinel-1	Radar	monitoring of peatland state
Millard et al. [44]	2018	Canada	temper- ate/northern	Vegetation indices	MODIS	Radar	monitoring soil moisture in peat- lands
Sencaki et al. [45]	2018	Sumatra	tropical	Machine learning land cover classifi- cation	Landsat 8 MODIS ASTER	Multispectral Radar	land classification / identification of peatlands
Torabi Haghghi et al. [46]	2018	Finland	boreal/northern	Vegetation indices	SPOT Landsat	Multispectral	changes in water conditions in the peatland
Asmuss et al. [47]	2019	German	temperate	Water table depth (WTD)	Sentinel-1	Radar	changes in water conditions in the peatland
Bandopadhyay et al. [48]	2019	Poland	temperate	Vegetation indices	Airborne data	Multispectral	peatland vegeta- tion mapping
Karlson et al. [49]	2019	Finland	boreal/northern	ArcticDEM ground de- formation	Sentinel-1	Radar	land classification / identification of peatlands
McPartland et al. [50]	2019	Alaska (USA) Minnesota (USA)	boreal/northern temperate	Vegetation indices	-	Multispectral	peatland vegeta- tion mapping changes in water conditions in the peatland
Räsänen et al. [51]	2019	Finland	boreal/northern	Vegetation indices	UAV (drone) Airborne data WorldView-2	Multispectral	peatland vegeta- tion mapping
Widyatmanti et al. [52]	2019	Indonesia	tropical	Vegetation indices Soil moisture indices	Landsat 8 Sentinel-2	Multispectral	monitoring soil moisture in peat- lands land classification
Yager et al. [53]	2019	Bolivia	temperate/oceanic	Supervised classification	Landsat 5 Landsat 8	Multispectral	monitoring of peatland state
Zhou et al. [54]	2019	Indonesia	tropical	InSAR ground deformation	ALOS	Radar	monitoring of peatland state
Bechtold et al. [55]	2020	Northern Hemisphere	-	Groundwater table (GWT) Soil moisture indices	SMOS	Radar	land classification / identification of peatlands changes in water conditions in the peatland
Burdun et al. [56]	2020	USA Canada Finland Sweden Estonia	temper- ate/northern	Soil moisture indices	Landsat MODIS	Multispectral	changes in water conditions in the peatland
Lees et al. [57]	2021	-	-	Vegetation indices Gross Primary	MODIS	Multispectral Radar	estimating carbon resources in peat- lands

Productivity						
Park et al. [58]	2020	Indonesia	tropical	Groundwater table (GWT) Soil moisture indices	MODIS	Hyperspectral estimating carbon resources in peatlands
Räsänen et al. [59]	2020	Finland	boreal/northern	Leaf-area index and biomass	UAV (drone)	Hyperspectral determination of biomass resources
Sencaki et al. [60]	2020	Sumatra	tropical	Machine learning land cover classification	Landsat 8 MODIS	Multispectral / identification of peatlands land classification
Sirin et al. [61]	2020	Moscow Region (Russia)	temperate	Supervised classification	SPOT Landsat Sentinel	Multispectral monitoring of peatland state
Sutikno et al. [62]	2020	Indonesia	tropical	Supervised classification	Landsat 8	Multispectral peatlands degradation
Zhang et al. [63]	2020	Florida (USA)	subtropical	Machine learning land cover classification	Landsat 8	Multispectral estimating methane balance
Amoakoh et al. [64]	2021	Ghana	tropical	Vegetation indices Texture features (moisture, roughness and shape) Machine learning land cover classification	Sentinel-2 Sentinel-1 Radar	Multispectral land classification / identification of peatlands
Anda et al. [65]	2021	Indonesia	tropical	Supervised classification	SPOT Landsat	Multispectral / identification of peatlands land classification
Anderson et al. [66]	2021	Bolivia Peru Argentina Chile	temperate/oceanic	Vegetation indices	Landsat	Multispectral monitoring of peatland state
Bandopadhyay et al. [67]	2021	Poland	temperate	Vegetation indices	Airborne data	Multispectral peatland vegetation mapping
Junttila et al. [68]	2021	Sweden Finland	boreal/northern	Vegetation indices	Sentinel-2 MODIS	Multispectral estimating CO2 balance Gross Primary Productivity

References

- USGS Landsat Available online: https://www.usgs.gov/core-science-systems/nli/landsat/landsat-8?qt-science_support_page_related_con=0#qt-science_support_page_related_con (accessed on 15 October 2021).

2. Dronova, I. Object-Based Image Analysis in Wetland Research: A Review. *Remote Sens.* **2015**, *7*, 6380–6413, doi:10.3390/rs70506380.
3. USGS Free, Open Landsat Data Unleashed the Power of Remote Sensing a Decade Ago Available online: <https://www.usgs.gov/center-news/free-open-landsat-data-unleashed-power-remote-sensing-a-decade-ago> (accessed on 15 October 2021).
4. USGS Landsat 9 Available online: <https://landsat.gsfc.nasa.gov/landsat-9> (accessed on 15 October 2021).
5. ESA Sentinel-1 SAR - Overview - Sentinel Online - Sentinel Online Available online: <https://sentinels.copernicus.eu/web/sentinel/user-guides/sentinel-1-sar/overview> (accessed on 15 October 2021).
6. ESA Sentinel-2 - Overview - Sentinel Online - Sentinel Online Available online: <https://sentinels.copernicus.eu/web/sentinel/missions/sentinel-2/overview> (accessed on 15 October 2021).
7. ESA SPOT 5 - Earth Online Available online: <https://earth.esa.int/web/eoportal/satellite-missions/s/spot-5> (accessed on 15 October 2021).
8. ESA SPOT 6 - Earth Online Available online: <https://earth.esa.int/eogateway/missions/spot-6> (accessed on 15 October 2021).
9. ESA SPOT 7 - Earth Online Available online: <https://earth.esa.int/eogateway/missions/spot-7> (accessed on 15 October 2021).
10. The European Space Agency Sentinel Available online: <https://sentinel.esa.int> (accessed on 5 May 2021).
11. Anderson, K.; Bennie, J.J.; Milton, E.J.; Hughes, P.D.M.; Lindsay, R.; Meade, R. Combining LiDAR and IKONOS Data for Eco-Hydrological Classification of an Ombrotrophic Peatland. *J. Environ. Qual.* **2010**, *39*, 260–273, doi:10.2134/jeq2009.0093.
12. Miettinen, J.; Liew, S.C. Degradation and Development of Peatlands in Peninsular Malaysia and in the Islands of Sumatra and Borneo since 1990. *Land Degrad. Dev.* **2010**, *21*, 285–296, doi:10.1002/ldr.976.
13. Neta, T.; Cheng, Q.; Bello, R.L.; Hu, B. Lichens and Mosses Moisture Content Assessment through High-Spectral Resolution Remote Sensing Technology: A Case Study of the Hudson Bay Lowlands, Canada. *Hydrol. Process.* **2010**, *24*, 2617–2628, doi:10.1002/hyp.7669.
14. Wijaya, A.; Reddy Marpu, P.; Gloaguen, R. Discrimination of Peatlands in Tropical Swamp Forests Using Dual-Polarimetric SAR and Landsat ETM Data. *Int. J. Image Data Fusion* **2010**, *1*, 257–270, doi:10.1080/19479832.2010.495323.
15. Connolly, J.; Holden, N.M.; Connolly, J.; Seaquist, J.W.; Ward, S.M. Detecting Recent Disturbance on Montane Blanket Bogs in the Wicklow Mountains, Ireland Using the MODIS Enhanced Vegetation Index. *Int. J. Remote Sens.* **2011**, *32*, 2377–2393, doi:10.1080/01431161003698310.
16. Frick, A.; Steffenhagen, P.; Zerbe, S.; Timmermann, T.; Schulz, K. Monitoring of the Vegetation Composition in Rewetted Peatland with Iterative Decision Tree Classification of Satellite Imagery. *Photogramm. - Fernerkund. - Geoinformation* **2011**, 109–122, doi:10.1127/1432-8364/2011/0076.
17. Harris, A.; Dash, J. A New Approach for Estimating Northern Peatland Gross Primary Productivity Using a Satellite-Sensor-Derived Chlorophyll Index. *J. Geophys. Res. Biogeosciences* **2011**, *116*, doi:10.1029/2011JG001662.
18. Jaenicke, J.; Englhart, S.; Siegert, F. Monitoring the Effect of Restoration Measures in Indonesian Peatlands by Radar Satellite Imagery. *J. Environ. Manage.* **2011**, *92*, 630–638, doi:10.1016/j.jenvman.2010.09.029.
19. Middleton, M.; Närhi, P.; Arkima, H.; Hyvönen, E.; Kuosmanen, V.; Treitz, P.; Sutinen, R. Ordination and Hyperspectral Remote Sensing Approach to Classify Peatland Biotopes along Soil Moisture and Fertility Gradients. *Remote Sens. Environ.* **2012**, *124*, 596–609, doi:10.1016/j.rse.2012.06.010.

20. Miettinen, J.; Hooijer, A.; Wang, J.; Shi, C.; Liew, S.C. Peatland Degradation and Conversion Sequences and Interrelations in Sumatra. *Reg. Environ. Change* **2012**, *12*, 729–737, doi:10.1007/s10113-012-0290-9.
21. Torbick, N.; Persson, A.; Olefeldt, D.; Frolking, S.; Salas, W.; Hagen, S.; Crill, P.; Li, C. High Resolution Mapping of Peatland Hydroperiod at a High-Latitude Swedish Mire. *Remote Sens.* **2012**, *4*, 1974–1994, doi:10.3390/rs4071974.
22. Akumu, C.E.; McLaughlin, J.W. Modeling Peatland Carbon Stock in a Delineated Portion of the Nayshkootayaow River Watershed in Far North, Ontario Using an Integrated GIS and Remote Sensing Approach. *CATENA* **2014**, *121*, 297–306, doi:10.1016/j.catena.2014.05.025.
23. O’Connell, J.; Connolly, J.; Holden, N.M. A Monitoring Protocol for Vegetation Change on Irish Peatland and Heath. *Int. J. Appl. Earth Obs. Geoinformation* **2014**, *31*, 130–142, doi:10.1016/j.jag.2014.03.006.
24. Watts, J.D.; Kimball, J.S.; Parmentier, F.J.W.; Sachs, T.; Rinne, J.; Zona, D.; Oechel, W.; Tagesson, T.; Jackowicz-Korczyński, M.; Aurela, M. A Satellite Data Driven Biophysical Modeling Approach for Estimating Northern Peatland and Tundra CO₂ and CH₄ Fluxes. *Biogeosciences* **2014**, *11*, 1961–1980, doi:10.5194/bg-11-1961-2014.
25. Cabezas, J.; Galleguillos, M.; Valdés, A.; Fuentes, J.P.; Pérez, C.; Perez-Quezada, J.F. Evaluation of Impacts of Management in an Anthropogenic Peatland Using Field and Remote Sensing Data. *Ecosphere* **2015**, *6*, 1–24, doi:10.1890/ES15-00232.1.
26. Crichton, K.A.; Anderson, K.; Bennie, J.J.; Milton, E.J. Characterizing Peatland Carbon Balance Estimates Using Freely Available Landsat ETM+ Data. *Ecohydrology* **2015**, *8*, 493–503, doi:10.1002/eco.1519.
27. Harris, A.; Charnock, R.; Lucas, R.M. Hyperspectral Remote Sensing of Peatland Floristic Gradients. *Remote Sens. Environ.* **2015**, *162*, 99–111, doi:10.1016/j.rse.2015.01.029.
28. Lehmann, J.R.K.; Münchberger, W.; Knoth, C.; Blodau, C.; Nieberding, F.; Prinz, T.; Pancotto, V.A.; Kleinebecker, T. High-Resolution Classification of South Patagonian Peat Bog Microforms Reveals Potential Gaps in Up-Scaled CH₄ Fluxes by Use of Unmanned Aerial System (UAS) and CIR Imagery. *Remote Sens.* **2016**, *8*, 173, doi:10.3390/rs8030173.
29. Bourgeau-Chavez, L.L.; Endres, S.; Powell, R.; Battaglia, M.J.; Benscoter, B.; Turetsky, M.; Kasischke, E.S.; Banda, E. Mapping Boreal Peatland Ecosystem Types from Multitemporal Radar and Optical Satellite Imagery. *Can. J. For. Res.* **2017**, *47*, 545–559, doi:10.1139/cjfr-2016-0192.
30. Connolly, J.; Holden, N.M. Detecting Peatland Drains with Object Based Image Analysis and Geoeye-1 Imagery. *Carbon Balance Manag.* **2017**, *12*, 7, doi:10.1186/s13021-017-0075-z.
31. Dissanska, M.; Bernier, M.; Payette, S. Object-Based Classification of Very High Resolution Panchromatic Images for Evaluating Recent Change in the Structure of Patterned Peatlands. *Can. J. Remote Sens.* **2017**, *35*, 189–215, doi:10.5589/m09-002.
32. Erudel, T.; Fabre, S.; Houet, T.; Mazier, F.; Briottet, X. Criteria Comparison for Classifying Peatland Vegetation Types Using In Situ Hyperspectral Measurements. *Remote Sens.* **2017**, *9*, 748, doi:10.3390/rs9070748.
33. Gatis, N.; Anderson, K.; Grand-Clement, E.; Luscombe, D.J.; Hartley, I.P.; Smith, D.; Brazier, R.E. Evaluating MODIS Vegetation Products Using Digital Images for Quantifying Local Peatland CO₂ Gas Fluxes. *Remote Sens. Ecol. Conserv.* **2017**, *3*, 217–231, doi:10.1002/rse2.45.
34. Gumbrecht, T.; Roman-Cuesta, R.M.; Verchot, L.; Herold, M.; Wittmann, F.; Householder, E.; Herold, N.; Murdiyarsa, D. An Expert System Model for Mapping Tropical Wetlands and Peatlands Reveals South America as the Largest Contributor. *Glob. Change Biol.* **2017**, *23*, 3581–3599, doi:10.1111/gcb.13689.
35. Hribljan, J.A.; Suarez, E.; Bourgeau-Chavez, L.; Endres, S.; Lilleskov, E.A.; Chimbolema, S.; Wayson, C.; Serocki, E.; Chimner, R.A. Multidate, Multisensor Remote Sensing Reveals High Density of Carbon-Rich Mountain Peatlands in the Páramo of Ecuador. *Glob. Change Biol.* **2017**, *23*, 5412–5425, doi:10.1111/gcb.13807.

36. Medvedeva, M.A.; Vozbrannaya, A.E.; Sirin, A.A.; Maslov, A.A. Capabilities of Multispectral Satellite Data in an Assessment of the Status of Abandoned Fire Hazardous and Rewetting Peat Extraction Lands. *Izv. Atmospheric Ocean. Phys.* **2017**, *53*, 1072–1080, doi:10.1134/S0001433817090201.
37. Merchant, M.A.; Adams, J.R.; Berg, A.A.; Baltzer, J.L.; Quinton, W.L.; Chasmer, L.E. Contributions of C-Band SAR Data and Polarimetric Decompositions to Subarctic Boreal Peatland Mapping. *IEEE J. Sel. Top. Appl. Earth Obs. Remote Sens.* **2017**, *10*, 1467–1482, doi:10.1109/JSTARS.2016.2621043.
38. Novresiandi, D.A.; Nagasawa, R. Polarimetric Synthetic Aperture Radar Application for Tropical Peatlands Classification: A Case Study in Siak River Transect, Riau Province, Indonesia. *J. Appl. Remote Sens.* **2017**, *11*, 016040, doi:10.1117/1.JRS.11.016040.
39. White, L.; Millard, K.; Banks, S.; Richardson, M.; Pasher, J.; Duffe, J. Moving to the RADARSAT Constellation Mission: Comparing Synthesized Compact Polarimetry and Dual Polarimetry Data with Fully Polarimetric RADARSAT-2 Data for Image Classification of Peatlands. *Remote Sens.* **2017**, *9*, 573, doi:10.3390/rs9060573.
40. Alshammari, L.; Large, D.J.; Boyd, D.S.; Sowter, A.; Anderson, R.; Andersen, R.; Marsh, S. Long-Term Peatland Condition Assessment via Surface Motion Monitoring Using the ISBAS DInSAR Technique over the Flow Country, Scotland. *Remote Sens.* **2018**, *10*, 1103, doi:10.3390/rs10071103.
41. Arroyo-Mora, J.P.; Kalacska, M.; Soffer, R.; Ifimov, G.; Leblanc, G.; Schaaf, E.S.; Lucanus, O. Evaluation of Phenospectral Dynamics with Sentinel-2A Using a Bottom-up Approach in a Northern Ombrotrophic Peatland. *Remote Sens. Environ.* **2018**, *216*, 544–560, doi:10.1016/j.rse.2018.07.021.
42. Kalacska, M.; Arroyo-Mora, J.P.; Soffer, R.J.; Roulet, N.T.; Moore, T.R.; Humphreys, E.; Leblanc, G.; Lucanus, O.; Inamdar, D. Estimating Peatland Water Table Depth and Net Ecosystem Exchange: A Comparison between Satellite and Airborne Imagery. *Remote Sens.* **2018**, *10*, 687, doi:10.3390/rs10050687.
43. Marshall, C.; Large, D.J.; Athab, A.; Evers, S.L.; Sowter, A.; Marsh, S.; Sjögersten, S. Monitoring Tropical Peat Related Settlement Using ISBAS InSAR, Kuala Lumpur International Airport (KLIA). *Eng. Geol.* **2018**, *244*, 57–65, doi:10.1016/j.enggeo.2018.07.015.
44. Millard, K.; Thompson, D.K.; Parisien, M.-A.; Richardson, M. Soil Moisture Monitoring in a Temperate Peatland Using Multi-Sensor Remote Sensing and Linear Mixed Effects. *Remote Sens.* **2018**, *10*, 903, doi:10.3390/rs10060903.
45. Sencaki, D.B.; Gandharum, A.; Dayuf, M.J.; Sumargana, L. Peatland Delineation Using Remote Sensing Data in Sumatera Island. In Proceedings of the 2018 Ieee Asia-Pacific Conference on Geoscience, Electronics and Remote Sensing Technology (agers); Ieee: New York, 2018; pp. 7–12.
46. Torabi Haghghi, A.; Menberu, M.W.; Darabi, H.; Akanegbu, J.; Kløve, B. Use of Remote Sensing to Analyse Peatland Changes after Drainage for Peat Extraction. *Land Degrad. Dev.* **2018**, *29*, 3479–3488, doi:10.1002/ldr.3122.
47. Asmuss, T.; Bechtold, M.; Tiemeyer, B. On the Potential of Sentinel-1 for High Resolution Monitoring of Water Table Dynamics in Grasslands on Organic Soils. *Remote Sens.* **2019**, *11*, 1659, doi:10.3390/rs11141659.
48. Bandopadhyay, S.; Rastogi, A.; Rascher, U.; Rademske, P.; Schickling, A.; Cogliati, S.; Julitta, T.; Mac Arthur, A.; Hueni, A.; Tomelleri, E.; et al. Hyplant-Derived Sun-Induced Fluorescence—A New Opportunity to Disentangle Complex Vegetation Signals from Diverse Vegetation Types. *Remote Sens.* **2019**, *11*, 1691, doi:10.3390/rs11141691.
49. Karlson, M.; Gålfalk, M.; Crill, P.; Bousquet, P.; Saunois, M.; Bastviken, D. Delineating Northern Peatlands Using Sentinel-1 Time Series and Terrain Indices from Local and Regional Digital Elevation Models. *Remote Sens. Environ.* **2019**, *231*, 111252, doi:10.1016/j.rse.2019.111252.
50. McPartland, M.Y.; Kane, E.S.; Falkowski, M.J.; Kolka, R.; Turetsky, M.R.; Palik, B.; Montgomery, R.A. The Response of Boreal Peatland Community Composition and NDVI to Hydrologic Change, Warming, and Elevated Carbon Dioxide. *Glob. Change Biol.* **2019**, *25*, 93–107, doi:10.1111/gcb.14465.

51. Räsänen, A.; Juutinen, S.; Tuittila, E.-S.; Aurela, M.; Virtanen, T. Comparing Ultra-High Spatial Resolution Remote-Sensing Methods in Mapping Peatland Vegetation. *J. Veg. Sci.* **2019**, *30*, 1016–1026, doi:10.1111/jvs.12769.
52. Widyatmanti, W.; Umarhadi, D.; Ningam, M.U.L.; Sarah, Z.; Nugroho, K.; Wahyunto; Sulaeman, Y. Mapping Acid Sulfate Soil Hydrogeomorphical Unit on the Peatland Landscape Using a Hybrid Remote Sensing Approach. In *Tropical Wetlands – Innovation in Mapping and Management: Proceedings of the International Workshop on Tropical Wetlands: Innovation in Mapping and Management*; Sulaeman, Y., Poggio, L., Minasny, B., Nursyamsi, D., Eds.; CRC Press: London, 2019; pp. 30–37 ISBN 978-0-429-26446-7.
53. Yager, K.; Valdivia, C.; Slayback, D.; Jimenez, E.; Meneses, R.I.; Palabral, A.; Bracho, M.; Romero, D.; Hubbard, A.; Pacheco, P.; et al. Socio-Ecological Dimensions of Andean Pastoral Landscape Change: Bridging Traditional Ecological Knowledge and Satellite Image Analysis in Sajama National Park, Bolivia. *Reg. Environ. Change* **2019**, *19*, 1353–1369, doi:10.1007/s10113-019-01466-y.
54. Zhou, Z.; Li, Z.; Waldron, S.; Tanaka, A. InSAR Time Series Analysis of L-Band Data for Understanding Tropical Peatland Degradation and Restoration. *Remote Sens.* **2019**, *11*, 2592, doi:10.3390/rs11212592.
55. Bechtold, M.; De Lannoy, G.J.M.; Reichle, R.H.; Roose, D.; Balliston, N.; Burdun, I.; Devito, K.; Kurbatova, J.; Strack, M.; Zarov, E.A. Improved Groundwater Table and L-Band Brightness Temperature Estimates for Northern Hemisphere Peatlands Using New Model Physics and SMOS Observations in a Global Data Assimilation Framework. *Remote Sens. Environ.* **2020**, *246*, 111805, doi:10.1016/j.rse.2020.111805.
56. Burdun, I.; Bechtold, M.; Sagris, V.; Lohila, A.; Humphreys, E.; Desai, A.R.; Nilsson, M.B.; De Lannoy, G.; Mander, Ü. Satellite Determination of Peatland Water Table Temporal Dynamics by Localizing Representative Pixels of A SWIR-Based Moisture Index. *Remote Sens.* **2020**, *12*, 2936, doi:10.3390/rs12182936.
57. Lees, K.J.; Artz, R.R.E.; Chandler, D.; Aspinall, T.; Boulton, C.A.; Buxton, J.; Cowie, N.R.; Lenton, T.M. Using Remote Sensing to Assess Peatland Resilience by Estimating Soil Surface Moisture and Drought Recovery. *Sci. Total Environ.* **2021**, *761*, 143312, doi:10.1016/j.scitotenv.2020.143312.
58. Park, H.; Takeuchi, W.; Ichii, K. Satellite-Based Estimation of Carbon Dioxide Budget in Tropical Peatland Ecosystems. *Remote Sens.* **2020**, *12*, 250, doi:10.3390/rs12020250.
59. Räsänen, A.; Juutinen, S.; Kalacska, M.; Aurela, M.; Heikkinen, P.; Mäenpää, K.; Rimali, A.; Virtanen, T. Peatland Leaf-Area Index and Biomass Estimation with Ultra-High Resolution Remote Sensing. *GIScience Remote Sens.* **2020**, *57*, 943–964, doi:10.1080/15481603.2020.1829377.
60. Sencaki, D.B.; Prayogi, H.; Arfah, S.; Pianto, T.A. Machine Learning Approach for Peatland Delineation Using Multi-Sensor Remote Sensing Data in Ogan Komering Ilir Regency. *IOP Conf. Ser. Earth Environ. Sci.* **2020**, *500*, 012005, doi:10.1088/1755-1315/500/1/012005.
61. Sirin, A.A.; Medvedeva, M.A.; Makarov, D.A.; Maslov, A.A.; Joosten, H. Multispectral Satellite Based Monitoring of Land Cover Change and Associated Fire Reduction after Large-Scale Peatland Rewetting Following the 2010 Peat Fires in Moscow Region (Russia). *Ecol. Eng.* **2020**, *158*, 106044, doi:10.1016/j.ecoleng.2020.106044.
62. Sutikno, S.; Hidayati, N.; Rinaldi; Nasrul, B.; Putra, A.; Qomar, N. Classification of Tropical Peatland Degradation Using Remote Sensing and GIS Technique. *AIP Conf. Proc.* **2020**, *2255*, 070022, doi:10.1063/5.0013881.
63. Zhang, C.; Comas, X.; Brodylo, D. A Remote Sensing Technique to Upscale Methane Emission Flux in a Subtropical Peatland. *J. Geophys. Res. Biogeosciences* **2020**, *125*, e2020JG006002, doi:10.1029/2020JG006002.
64. Amoakoh, A.O.; Aplin, P.; Awuah, K.T.; Delgado-Fernandez, I.; Moses, C.; Alonso, C.P.; Kankam, S.; Mensah, J.C. Testing the Contribution of Multi-Source Remote Sensing Features for Random Forest Classification of the Greater Amanzule Tropical Peatland. *Sensors* **2021**, *21*, 3399, doi:10.3390/s21103399.

65. Anda, M.; Ritung, S.; Suryani, E.; Sukarman; Hikmat, M.; Yatno, E.; Mulyani, A.; Subandiono, R.E.; Suratman; Husnain Revisiting Tropical Peatlands in Indonesia: Semi-Detailed Mapping, Extent and Depth Distribution Assessment. *Geoderma* **2021**, *402*, 115235, doi:10.1016/j.geoderma.2021.115235.
66. Anderson, T.G.; Christie, D.A.; Chávez, R.O.; Olea, M.; Anchukaitis, K.J. Spatiotemporal Peatland Productivity and Climate Relationships Across the Western South American Altiplano. *J. Geophys. Res. Biogeosciences* **2021**, *126*, e2020JG005994, doi:10.1029/2020JG005994.
67. Bandopadhyay, S.; Rastogi, A.; Cogliati, S.; Rascher, U.; Gąbka, M.; Juszczak, R. Can Vegetation Indices Serve as Proxies for Potential Sun-Induced Fluorescence (SIF)? A Fuzzy Simulation Approach on Airborne Imaging Spectroscopy Data. *Remote Sens.* **2021**, *13*, 2545, doi:10.3390/rs13132545.
68. Junntila, S.; Kelly, J.; Kljun, N.; Aurela, M.; Klemedtsson, L.; Lohila, A.; Nilsson, M.B.; Rinne, J.; Tuittila, E.-S.; Vestin, P.; et al. Upscaling Northern Peatland CO₂ Fluxes Using Satellite Remote Sensing Data. *Remote Sens.* **2021**, *13*, 818, doi:10.3390/rs13040818.